Proceedings of the 6th International Conference on the Application of Physical Modelling in Coastal and Port Engineering and Science (Coastlab16)
Ottawa, Canada, May 10-13, 2016
Copyright ©: Creative Commons CC BY-NC-ND 4.0

ANALYSIS OF POST OVERTOPPING FLOW IMPACTS ON A VERTICAL WALL AT THE BELGIAN COAST

MAXIMILIAN STREICHER[1], ANDREAS KORTENHAUS[1], CORINNA HOHLS[2]

1 Dept. of Civil Engineering, Ghent University, Technologiepark 904,
B-9052 Zwijnaarde (Ghent), Belgium; email: Maximilian.Streicher@UGent.be
2 Leichtweiß-Institut for Hydraulic Engineering and Water Resources, TU Braunschweig, Beethovenstraße 51a,
D-38106 Braunschweig, Germany; email: Corinna.Hohls@tu-braunschweig.de

ABSTRACT

This study comprises the analysis of bores, arising from overtopped waves at sea dikes and the subsequent impacts on a vertical wall at the end of the promenade on top of the dike. Physical experiments were conducted in the wave flume facility at Ghent University. Layer thicknesses, velocities and the impact forces on the storm wall were measured. Whereas the overtopping of storm walls is a well described phenomena, the actual loads causing potential damages on the storm wall, remain less well investigated. In this study, three different impact types based on the force signal shape were distinguished and related to bore characteristics using video analysis. The different impact types were named 'quasi-static/down-rush bore impact', 'dynamic bore impact' and 'pulsating bore impact'. A large amount (86%) of the impacts were assigned to the 'quasi-static/down-rush bore impacts' type with a double peak force shape and a dominant second force peak. Furthermore, the layer thicknesses and velocities of the bore on the promenade were compared to the measured forces at the wall for individual impacts. It became clear from this analysis that the layer thickness in front of the wall showed the best correlation to the forces on the wall.

KEYWORDS: overtopping bore, storm wall, impact force, velocities, layer thickness, run-up

1 INTRODUCTION AND OBJECTIVES

The coastal area worldwide is comparably densely populated and in 2000 half of the major cities counting more than 500,000 inhabitants are located within 50 km of the coastline (UNEP, 2006). The attractiveness of the coast leads to an increased number of buildings and assets close to the coastline. At the same time, the sea level rises and an increased storminess is expected in the future. As projected in the latest synthesis report of the intergovernmental panel on climate change (IPCC) the global sea mean level rise will exceed the observed rate of 2 mm/year (1971-2010) in the 21st century (IPCC, 2014). When vulnerability in the coastal area and probability for flooding increase, the risk for inhabitants, accompanying industry and infrastructure also goes up. This is especially true for countries with low topographies compared to the sea level, such as Belgium.

It was shown that 1/3 of the Belgium coastline is not properly protected against severe storm surges (Mertens et al., 2008). Structural coastal protection measures, such as dikes and storm walls, are commonly designed and assessed based on a reduction in overtopping (Verwaest et al., 2011), not taking into account the hydrodynamic loads by overtopped waves. Overtopped wave loads on storm walls, buildings and people have scarcely been measured resulting in a lack of generic design guidance (Eurotop, 2007). Overtopping wave loads can be a severe hazard to people and objects exposed. Geeraerts et al. (2005) found overtopped wave loads on a dummy person to be 8.8 kN, with accompanying overtopping of $q < 1$ l/s/m. This is a rather high value compared to a 140 N slipping limit for pedestrians proposed by Endoh and Takahashi (1994). Allsop et al. (2005) pointed out that the loads due to overtopped waves can be very large and are not negligible.

Along the coasts of low-lying countries, buildings are constructed at the end of wide-crested dikes or revetments, like in Belgium. This setting makes it possible for turbulent bores, which result from waves running up and overtopping the crest, to

cause severe impacts on these structures. The loads due to the impact of the these bores need to be predicted to enable a reliable design and protection from failure. The physical processes and conditions of bore formation and their variation over the promenade to final interaction with a secondary defense structure or building are barely investigated and not completely understood (Allsop et al., 2004). Hence, this study focuses on the analysis of such impacts on the storm wall, situated on top of a dike. Furthermore the bore characteristics (layer thickness and velocity) are analyzed and correlated with the force on the wall. This will enhance the understanding of post overtopping flows and impact behavior on a storm wall. Specified objectives are as followed: (1) to identify typical impact types of a bore hitting the storm wall by analysis of the force signal; (2) to relate the impact types to bore characteristics by the help of video analyses; (3) to study the layer thickness and velocity of the bores; and (4) to correlate layer thickness and velocity with the force.

2 PREVIOUS RESEARCH

Layer thicknesses and velocities of overtopping flows on seaside promenades were experimentally and theoretically determined for a set-up without a wall on the promenade (Hughes et al., 2012; Schüttrumpf and Oumeraci, 2005). They found that the maximum velocity did not necessarily coincide with the maximum layer thickness of the overtopping flow. Also, they point out that maximum velocities are measured at the front of the overtopping flow. This was supported by Van der Meer et al. (2010) stating that the front velocities represented well the maximum velocity averaged over the depth.

The influence of a wall on the post overtopping flow was studied by Chen et al. (2015). The term 'wall effect' was used to describe the effects of the wall on the flow. This was the reflection of the flow at the wall and its interaction with subsequent incoming flows. They found that the overtopping flow and the final impact at the wall was comparable to tsunami bore impacts on buildings or broken overtopped wave impacts on storm walls on top of rubble mound break waters.

Bubble image velocimetry was used by Chen et al. (2014) to extract velocity information from the turbulent bore passing over the promenade. Interaction and wet-bed scenarios were distinguished and the analysis done for the latter one. 4 stages of impact were defined: (1) during pre-impact the bore was travelling and transforming over the promenade. After that (2) initial impact was assigned from first impact of the bore tip jet over the impact of the main water body until (3) continued deflection lead to upward movement of the water mass. During reflection (4) the upward deflected water started to fall and due to blocking of the wall travelled in the opposite direction.

Bore characteristics and impacts in a wave flume were studied by Ramsden (1996) using a laser-induced fluorescence system to record the incoming bore profiles. They distinguished undular and strong turbulent bore types. The main difference was the bore front which became steeper and more turbulent in the latter case. The steeper the bore front became the larger run-up and impact forces were measured. Based on the run-up on the wall and the hydrostatic load they derived an empirical formula to predict the forces on the wall. Additionally they found that the maximum run-up height did not coincide with the maximum quasi-static force peak, but occurred earlier in time.

Prototype tests of overtopped wave loads on a vertical wall were carried out by (De Rouck et al., 2012; Ramachandran et al., 2012) in the 'Grosser Wellenkanal' (GWK) Hannover. The layer thickness of the bore was determined by a wave gauge located on the promenade. The velocity was obtained by the time the bore traveled from one wave gauge to the next on the promenade. Knowing the distance between the wave gauges, an average speed could be obtained. It was found that multiplying the maximum layer thickness and velocity gave the best correlation with the measured force. They noticed a stochastic behaviour of the measured forces between tests with identical conditions. Possible reasons were turbulences on the promenade, interactions of incoming waves with reflected waves, residual water layers on the promenade, and air entrainment in the overtopping waves.

A test campaign featuring the overtopping simulator to model the impact of overtopping wave volumes on a storm wall was conducted by Van Doorslaer et al. (2012). Flow depths and flow velocities were measured by means of a potentiometer and paddle wheels respectively. An empirical relationship between the measured flow depth, velocity, and the load on the storm wall was found.

In most studies a double peak impact shape was observed in the force signal (Chen et al., 2012; Chen et al., 2014; De Rouck et al., 2012; Ramachandran et al., 2012). It can be compared to the double peak shape described in Kortenhaus and Oumeraci (1998) to classify wave loading on vertical structures. The first peak is typically assigned to a dynamic impact of the moving bore being blocked by the structure. During deflection and reflection of the bore a dominant influence of the second peak is observed. The physical reason for the second peak is discussed controversially. It is either assigned to a hydrostatic force, due to the water in front of the wall (De Rouck et al., 2012) or to the down-rush of water after run-up and blocking of the wall in one direction (Chen et al., 2012; Martin et al., 1999; Ramsden, 1996). The latter argued that the second force peak is situated after the maximum run-up in time and therefore cannot be directly assigned to a maximum water layer in front of the wall.

3 EXPERIMENTAL SET-UP

Physical experiments were conducted in the 30 m long, 1.2 m high and 1 m wide wave flume at Ghent University in March 2015. The waves were generated by a piston type wave paddle equipped with a 1st order reflection compensation mechanism (Figure 2a). The wave paddle took 3.15 m of the flume length, therefore an operational length of about 27 m can be used. This was a decisive factor since a gentle foreshore to accurately model the wave transformation processes was constructed (Figure 2b). The foreshore had a slope of 1:35, followed by the dike with a 1:2 slope. Additionally a 10 m wide promenade in prototype scale was attached to the dike crest (Figure 1). The crest elevation and water level were varied resulting in freeboards R_c between 1 m – 3 m. The scale of the model tests was 1:25. The foreshore was built of concrete and the dike and promenade were constructed in wood. The test set-up was varied slightly by removing the wall on the promenade to measure the undisturbed flow characteristics of bores on the promenade.

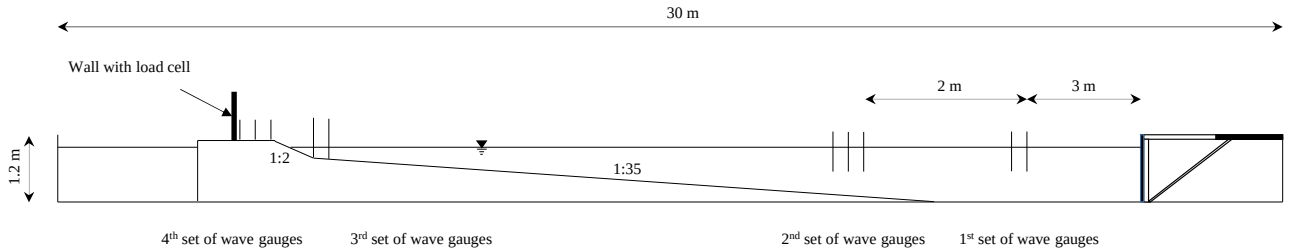

Figure 1: Cross section of wave flume with model set-up

An irregular Jonswap wave spectrum with peak enhancement factor $\gamma = 3.3$ was used during the tests. An offshore wave spectrum with 1000 waves was created with different spectral wave heights H_s between 2 m and 4.75 m (prototype units). Related peak wave periods T_p ranged between 8.5 s and 13.2 s. The resulting spectral wave heights at the dike toe ranged between 0.53 m and 2 m (Table 1). Due to wave breaking on the shallow foreshore long waves were found at the dike toe location.

Table 1. Experimental set-up. Model and wave parameters (prototype units)

Scale	H_s	T_p	h_{off}	h_{toe}	R_c	α	m	B
[-]	[m]	[s]	[m]	[m]	[m]	[-]	[-]	[m]
1:25	2-4.75	8.5-13.2	16.3-17.3	0.3-1.3	1-3	1:2	1:35	10

Measurements of the waves were taken at four locations along the flume. The recording system DHI Wave Amplifier 102E was used, including typical resistance type wave gauges. The 1st set of wave gauges was located near the paddle and served as an input for the active wave absorption system of the paddle. The 2nd set consisted of three wave gauges and was installed in an offshore location and was used to distinguish incident and reflected waves using the method of Mansard and Funke (1980). The 3rd set of wave gauges was set-up at the dike toe location and provided the necessary information about

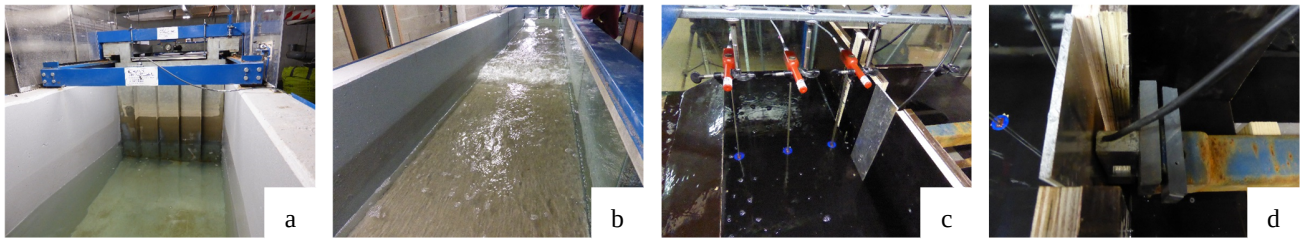

Figure 2: Piston wave paddle (a), waves breaking on shallow foreshore (b), the geometrical set-up dike-promenade-wall is equipped with flash-mounted layer thickness gauges and metal measurement plate attached to a load cell (c), rigid support of load cell and measurement plate to the back of the flume (d)

water elevation in front of the dike structure. It consisted of two gauges placed in flume direction 0.15 m apart from each other. The 4th set of wave gauges was flush mounted on top of the promenade (Figure 2c). The first wave gauge on the promenade was 0.05 m, the second one 0.2 m and the third one 0.35 m landwards of the crest, respectively. The third wave gauge was also mounted 0.05 m in front of the wall. The sampling frequency of the gauges was 40 Hz. The wall itself was

equipped with a 3 kg load cell of the 1042 model by Tedea-Huntleigh. The width of the measurement plate attached to the load cell was 0.1 m and the load cell was supported by a steel beam fixed to the end of the flume to provide a very stiff structure (Figure 2d). To measure the forces a strain gauge, bonded to the load cell, was used to convert the deformation force into an electrical signal. The electrical resistance of the strain gauge will change based on mechanical deformation. For the load cell a sampling frequency of 1000 Hz was used, known to provide robust enough results (Oumeraci et al., 1993).

4 ANALYSIS AND RESULTS

4.1 Methodology

11 tests with different dike heights, wave and water level parameters were chosen for analysis. They all had in common that from initially 1000 waves only a certain number overtopped the dike crest and led to a post overtopping bore, which eventually impacted the wall at the end of the promenade. This study focuses on the characterization of post overtopping flow impacts. Hence it is relevant to describe the selection of bores for the analysis but not the chain of parameters leading to the creation of the same (e.g. foreshore slope, dike slope, dike height, freeboard, wave parameter, etc.). When selecting bores for further analysis a semi-automatic approach using the MATLAB® software was applied. For better comparison, the signal of the layer thickness gauges on the promenade, the load cell signal, and the video recording were synchronized in time. From the synchronized measurements only bores were selected which actually created an impact at the vertical wall. This impact had to exceed a value of 0.5 N in model scale and is therefore equivalent to the hydrostatic force created by a 0.01 m water layer in front of the wall. This is also sufficient to clearly distinguish the impact from any noise in the force signal. Due to the complex interactions of incoming and reflected bores on the promenade only discrete bores were chosen for the analysis. Discrete in this context describes either a single bore approaching the promenade or the first bore of a group of bores. No residual water layer on the promenade and no reflected bores were included in this analysis. A maximum of 0.005 m residual water layer on the promenade is allowed for a minimum of 1.5 s in order to select the next bore for analysis. The chosen thresholds and limitations for the discreet bore were expected to be on the safe side, since residual water layers on the promenade and interactions with reflected bores should damp the energy of the incoming bores. The chosen bores were approved by manually checking the conditions for each event from force and layer thickness measurement. The selection procedure as described above is summarized in Figure 3. In total, 776 individual bore impacts remained after this selection process for further analysis, including the ones related to the highest measured impacts.

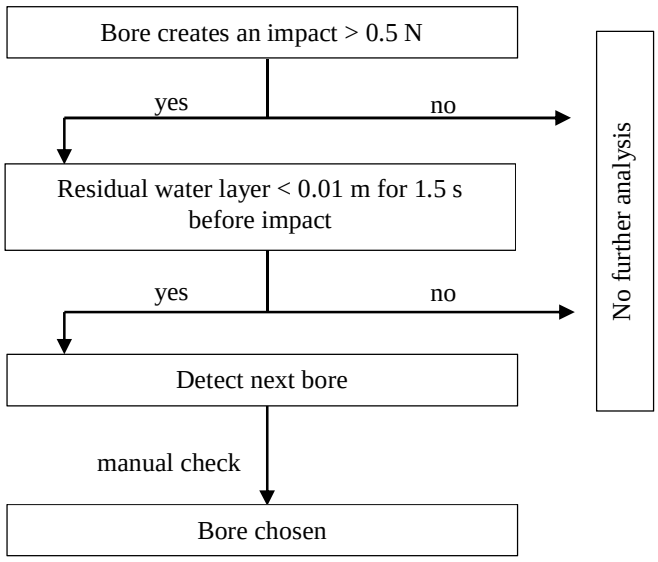

Figure 3: Selection procedure of bores for analysis (measures in model scale)

4.2 Impact case

The analysis of the force signal is done using the L~Davis software package. A timeframe for analysis is assigned to each test and an individual frequency filter defined. The goal is to filter out all frequencies which cause noise in the signal. The noise in the signal is caused by high frequencies. The band of high frequencies is filtered out in the frequency domain and a smoother signal is the result. At the same time the signal should keep its original shape and dimension as best as possible. In general, detecting the highest values is important since these have the highest impact on buildings and storm walls. Hence, the peak values after filtering were obtained for the selected bores. The load cell is attached to a 0.1 m wide metal plate. The total force values were therefore divided by the width of the plate in order to receive the force per meter width. Especially, for low impacts it is not obvious to distinguish a peak caused by an impact and noise. A video comparison showed that the selected events above 0.5 N are easily distinguishable from the noise in the signal. Typically the force signal has a double peak shape.

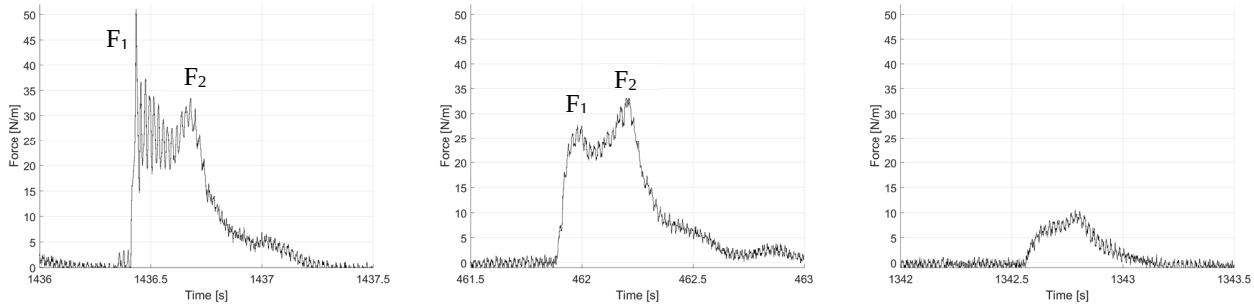

Figure 4: Impact cases of load cell measurement. 'Dynamic bore impact' (left), 'quasi-static/down-rush bore impact' (middle) and 'pulsating bore impact' (right)

The first peak is commonly referred to as dynamic impact force and linked to high speed and steep slope of the impacting bore (Ramsden, 1996). Whereas the second peak is referred to as the quasi-static impact force and linked to the hydrostatic pressure of the water layer in front of the wall. Although there are other approaches in literature saying that the second peak may result from the down-rush of the water after maximum run-up (Ramsden, 1996), also referred to as reflecting pressure or down-rush impact. This question can only be resolved with fully synchronized run-up and force measurements to better understand the correlation between fluid motion and impact histories near the wall. The double peak shape of the force signal is subdivided into two cases where either the 1st or the 2nd peak is higher (Figure 4, left and middle). Since only the maximum force values are retrieved by the Ldavis software, the information whether the maximum force is found at the 1st or 2nd peak is of importance because of the different underlying physical processes. The distinction will facilitate the analysis and theoretical description of impact forces at vertical walls. If the ratio F_1 over F_2 would exceed the value of 1.2 the impact case is considered 'dynamic bore impact'. For all lower ratios the impact case is considered 'quasi-static/down-rush bore impact'. A third type of force signal shape is identified where no distinct peak is detected and a rather smooth ascending and descending trend is observed (Figure 4, right). This type is referred to as 'pulsating bore impact'. In total the analysis is based on 776 individual impacts, where 6% are considered 'dynamic bore impacts'. The majority of 86% is considered 'quasi-static/down-rush bore impacts'. The remaining 8% are assigned to 'pulsating bore impacts' (Figure 5). For the 'dynamic bore impacts' a high frequency oscillation of the signal after the first impact is observed. This is probably due to pulsating air bubbles entrapped between the impinging wave and the wall, which are compressed by the subsequent flow. The presence of such air bubbles can only be validated by video analysis. Another reason for the oscillation in the signal could be related to the Eigen frequency of the structure which is not filtered out from the signal.

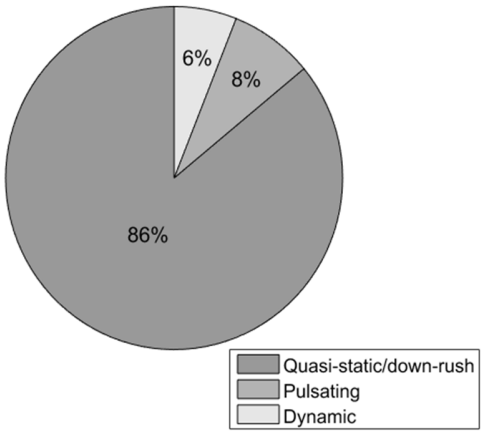

Figure 5: Distribution of bore impact cases

4.2 Bore type identification

From the force signal three different impact cases were distinguished. Knowing the time signal of the impacts, the related video sequence was found and analyzed with the objective to look for differences between the 'dynamic bore impact', 'quasi-static/down-rush bore impact' and 'pulsating bore impact' case. The studied criteria were the bore front steepness and run-up characteristics, air entrainment between wall and impinging bore, as well as the volume of the water body.

First, the 'quasi-static/down-rush bore impacts' were studied. Since they comprise the majority of impacts (667 events), only selected video analysis was performed. The related video sequence to Figure 4 (middle) is displayed in Figure 6. The impact stages were comparable to the one presented by Chen et al. (2014). During pre-impact, the bore was travelling and transforming over the promenade (Figure 6a). Followed by the initial impact of the bore tip until the impact of the main water body (b). The foamy bore front is impinging against the wall, compressed continuous deflection leads to an upward movement of the water mass (c and d) until the water starts to fall (e) and due to blocking of the wall moves in the opposite direction again (f). This is a rather typical behavior of the post overtopping flows and turbulent bores.

The 46 'dynamic bore impacts' were analyzed next. The frames extracted from video analysis for the dynamic impact in Figure 4 (left) are displayed in Figure 7. The most striking difference to the 'quasi-static/down-rush bore impacts' described

above was that the main water body of the incoming bore was interacting with the already reflected bore tip. The reflected tip of the bore is seen in Figure 7(a). The main water body was then deflected upwards already before the wall (b) and breaking against the wall under inclusion of an air pocket (c and d) was observed. The process of wave breaking including entrapped air, is comparable to plunging wave breaking at a vertical wall and the according dynamic force shape as described by Oumeraci et al. (1993). This phenomena was found to be the case for 73% of the 'dynamic bore impacts'. The remaining 'dynamic bore impacts' (27%) which showed no interaction with a reflected bore tip and were related to high velocities of

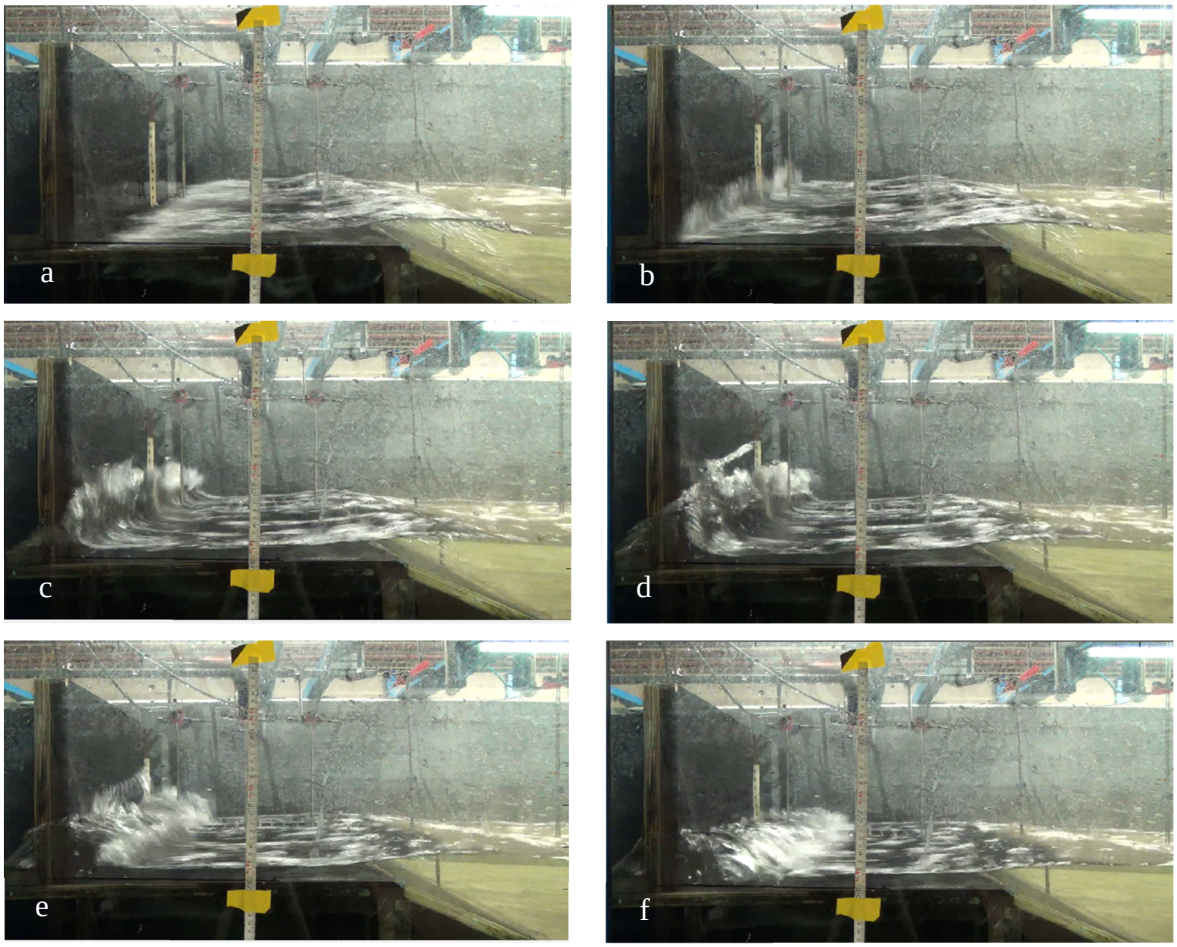

Figure 6: Turbulent bore related to 'quasi-static/down-rush bore impacts' (time between frames 0.08s, 12.5 Hz)

the incoming bore, a steep bore front and large layer thickness. In addition, the bores related to 'dynamic bore impacts' follow the same order of processes: transformation over the promenade (a), initial and main impact on the wall (c), compression and upward deflection (d), falling water body and reflection (e and f) in the opposite direction as described for 'quasi-static/down-rush bore impacts'.

The third impact case, 'pulsating bore impacts', were mainly related to shallow layer thicknesses. The slope of the bore front became very gentle and was hardly different from the slope of the following water body. The bore was approaching the wall and rose smoothly upwards, was deflected and reflected in one movement. No falling water masses were observed and the bore was able to travel freely in the opposite direction again. This also meant that no subsequent water was passing over the crest which would have pushed the water mass a longer time against the wall. It must be said, that the transition from bores related to 'quasi-static/down-rush bore impacts' and 'pulsating bore impacts' was rather smooth and sometimes hard to distinguish from the video signal alone. Therefore it seemed necessary to consider more parameters in order to better classify these three bore types. Here the analysis of layer thicknesses and velocities of the bores become important.

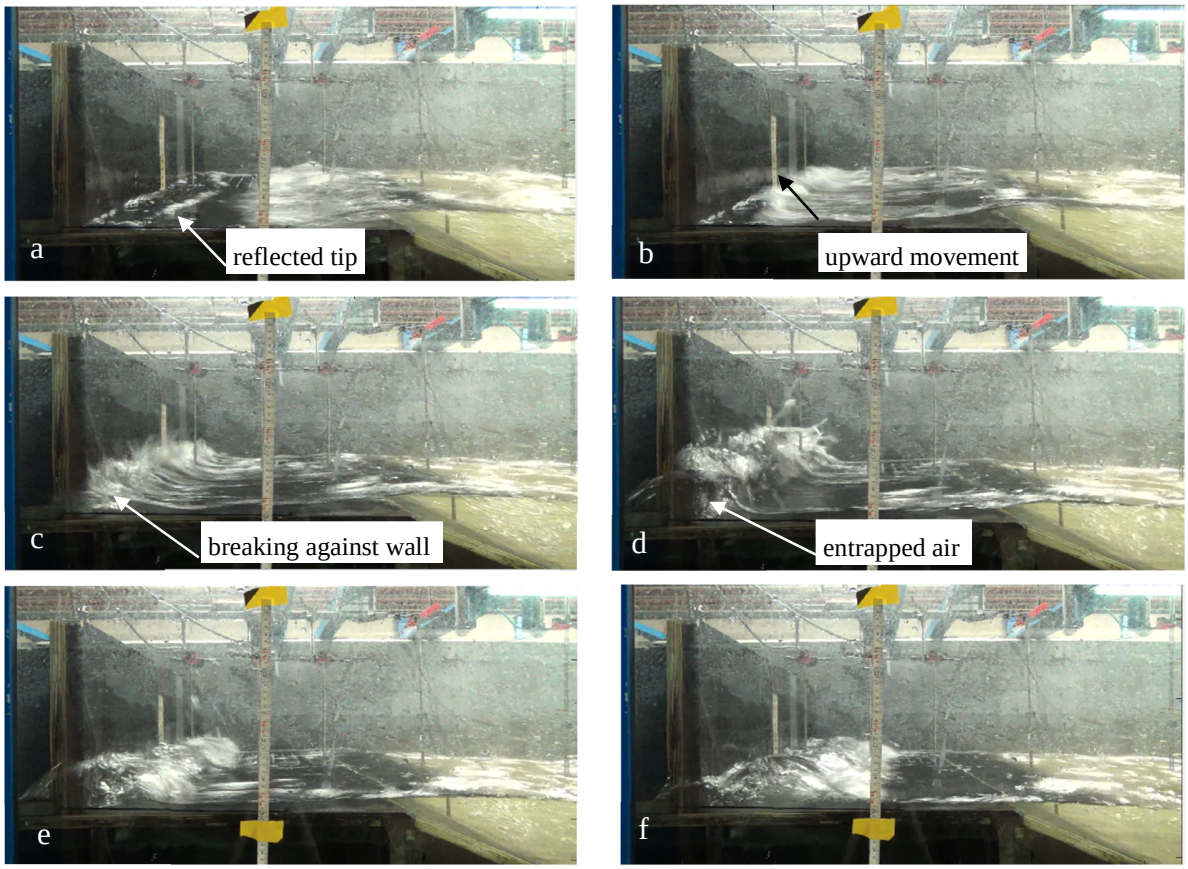

Figure 7: Plunging turbulent bore related to 'dynamic bore impacts' (time between frames 0.12 s, 12.5 Hz)

4.3 Layer thickness and velocity

The layer thickness was measured by resistance type wave gauges flush-mounted along the promenade. In total three gauges were installed from the crest until the wall, numbered WG 1 to WG 3, respectively. The layer thickness was measured for unobstructed flow (no wall installed on the promenade) and obstructed flow (wall installed on the promenade). This means the identical wave spectrum was repeated and the only difference between the tests was the presence (obstructed flow) or absence (unobstructed flow) of the wall. Measurements for a single bore at time 1046 s are displayed in Figure 8 for

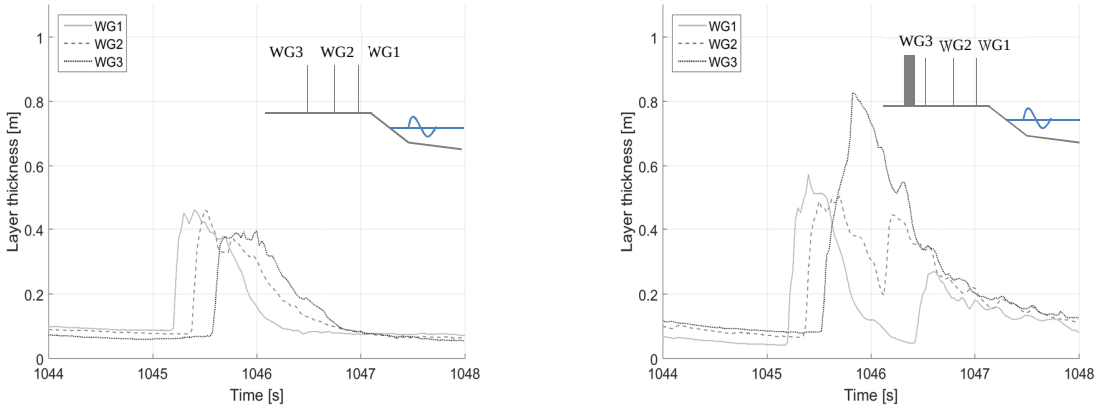

Figure 8: Layer thickness measurements for unobstructed (left) and obstructed (right) flow

unobstructed (left) and obstructed flow (right). All values are given in prototype scale. It can be seen that for the set-up without wall the layer thickness decreased from WG 2 to WG 3 whereas for the set-up with the wall an increasing trend between WG 2 and WG 3 was observed. The signal was almost 50% larger at WG 3 than for the first two wave gauges. WG 3 was

installed 0.05 m (model units) in front of the wall and is therefore measuring a mix of wave run-up at the wall and layer thickness. Also the reflected bore was observed first at WG 2 and finally at WG 1, with a decreasing trend. To retrieve the values for layer thickness and velocity from the measurement a semi-automatic approach was applied. For the 776 selected events (section 4.1) the time signals of WG 1 to WG 3 are displayed. Then the beginning of each bore and the maximum peak of each bore were clicked manually and the obtained Cartesian coordinates were transformed in to a time (x-axis) and layer thickness (y-axis) signal. The maximum peak of each event was then defined as layer thickness of the bore. The distance between two wave gauges was divided by the time the bore front needs to travel from one wave gauge to the other, in order to obtain the average velocity. It should be noted that manually identifying the beginning of the bore front was sometimes difficult due to a smooth rise and inconsistencies in the signal, probably induced by the foamy bore front and spray generated. The obtained layer thickness for WG 3 (0.05 m in front of the wall) and the average velocity between WG 2 and WG 3 for obstructed flow were plotted against the related force values. Following the classification in section 4.2 the plotted points were subdivided into the three bore impact types. The results are given in Figure 9.

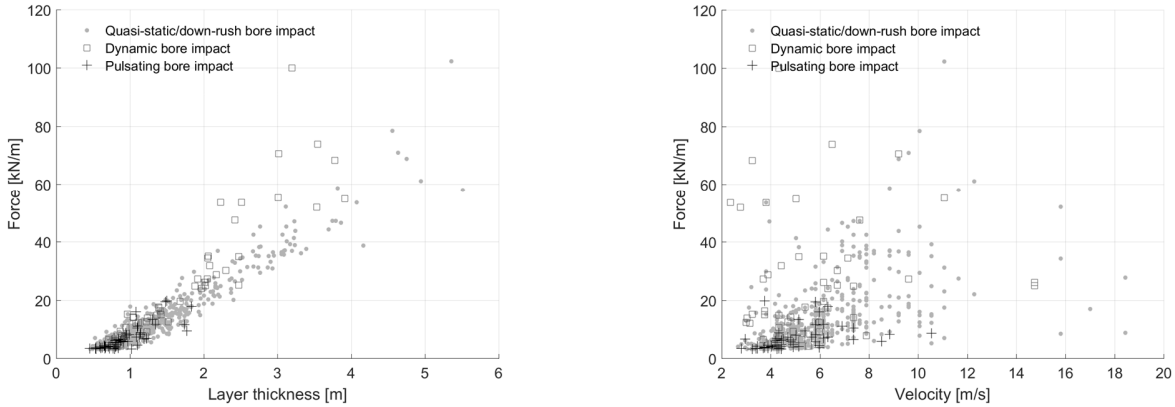

Figure 9: Correlation of layer thickness at the wall and bore impact force (left), velocity and bore impact force (right), in prototype units

The layer thickness at the wall correlates well with the impact force and it can be seen that 'pulsating bore impacts' are only present for a layer thickness below 2 m. They follow the same trend as 'quasi-static/down-rush bore impacts' and 'dynamic bore impacts' in this region. Above this threshold no more 'pulsating bore impacts' are found and the 'dynamic bore impacts' tend to be larger than the 'quasi-static/down-rush bore impacts'. Since they are physically based on the first impact of the bore against the wall, there might be a missing component, e.g. the incoming velocity, resulting in an upward shift of force values, or due to the breaking against the wall, as observed for 73% of the 'dynamic bore impacts'. Although the 'dynamic bore impacts' tended to be larger than the 'quasi-static/down-rush bore impacts', they were only present until a layer thickness of 4 m in front of the wall. All impacts above this critical value are 'quasi-static/down-rush bore impacts'. The maximum impact force is related to a 'quasi-static/down-rush bore impact' and a layer thickness at the wall of 5.5 m. This leads to the conclusion that there is a threshold above which the impact is solely dependent on the layer thickness at the wall. The correlation between velocity of the incoming bores and the forces is very poor and a large scatter is observed. The same result is obtained when motion tracking of the bore front for the video sequences was carried out. Either an improved measurement method needs to be elaborated or the velocity does not help to describe the impact force. The latter assumption might be supported by the fact, that all 'quasi-static/down-rush bore impacts' occur at the second peak of the force signal, meaning they are correlated to the layer thickness at the wall or down-rush and not with the incoming velocity anymore. Also, 73% of the 'dynamic bore impacts' were related to cases with plunging breaking against the wall, due to interactions with the reflected bore tips, upward deflections and breaking against the wall (section 4.3). This means there was another physical process present, independent of the incoming velocity. Following the good correlation between layer thicknesses and impact forces a theoretical hydrostatic force was calculated.

$$F_{theoretical} = \frac{1}{2} * \rho * g * h^2 \quad (1)$$

where:

ρ = density of water = 1000 [kg/m³]

g = gravitational acceleration = 9.81 [m/s²]

h = layer thickness in front of the wall [m].

The measured impact force is then plotted against the theoretical impact force calculated by Equation (1). Where between 0.03 kN and 25 kN the measured and calculated forces correlated well (Figure 10). For larger values the 'quasi-static/down-rush bore impacts' were underestimated by the hydrostatic calculation implying that there was a force term missing. This is probably due to the fact that the layer thickness was measured 0.05 m in front of the wall and not directly at the wall, where there was higher run-up expected. Another reason might be that the down-rushing water, after maximum run-up, induced a force on the wall as well which was measured but not accounted for in the hydrostatic calculation. As expected the higher 'dynamic bore impacts' were not well described by the hydrostatic force calculation and showed a larger scatter for values above 25 kN. It should be acknowledged that especially for 'dynamic bore impacts' the magnitude of the measured and then

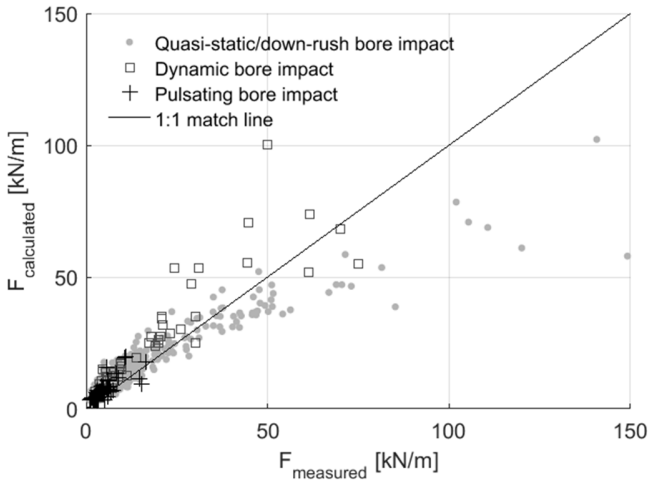

Figure 10: Measured and calculated bore impact force

scaled force values is likely to be overestimated due to less air entrained in the impacting bore compared to prototype dimensions (Cuomo et al., 2010). Additionally, model effects (e.g. smooth dike/promenade and perpendicular wave attack to coastline) lead as well to an overestimation of force magnitudes.

5 DISCUSSION AND OUTLOOK

Physical experiments were conducted and post overtopping bore characteristics and impacts at a vertical wall were analysed. In total 776 individual bores were selected and the synchronized layer thickness, force and video measurement investigated. Three different impact types were distinguished. The majority of force signals showed a double peak shape (92%) which was also stated in literature (Chen et al., 2014; De Rouck et al., 2012; Ramachandran et al., 2012). The double peak signals were subdivided in to 'dynamic bore impact' (dominant first peak) and 'quasi-static/down-rush bore impact' (dominant second peak). The majority of bore impacts at vertical walls and buildings, however, were comprised of 'quasi-static/down-rush bore impacts' (86%). Whether the second peak was directly related to a maximum layer thickness at the wall or to the down-rush of water can only be resolved with highly synchronized layer thickness and force measurements. Only 8% of the signal did not show any distinct force peak and was named 'pulsating bore impact'.

Video analysis of the different bore types were performed and the impact stages were comparable to the 4 impact stages found by Chen et al. (2014): transformation over the crest (1), initial and main impact (2), upward deflection (3), falling of water and reflection (4). Additionally 72% of the 'dynamic bore impacts' were explained by plunging bores breaking against the wall and inclusion of air. The breaking was initiated by interaction of the bore with an already reflected bore tip, upward movement and breaking against the wall.

The correlation of the layer thickness at the wall and resulting forces showed that there was a critical layer thickness of 2 m below which 'dynamic bore impacts', 'quasi-static/down-rush bore impacts', and 'pulsating bore impacts' followed the same trend. Between 2 m and 4 m layer thickness the 'dynamic bore impacts' were generally higher than the 'quasi-static/down-rush bore impacts' and above 4 m layer thickness only 'quasi-static/down-rush bore impacts' were found. Maximum forces were found for 'quasi-static/down-rush bore impacts' and layer thicknesses above 4 m. Hence, a theoretical force on the wall based on the hydrostatic pressure, induced by the layer thickness at the wall, was calculated.

The influence of velocities on the measured forces my increase for smaller promenade widths. Therefore experimental tests for varying promenade widths are recommended. Additionally, an improved velocity measurement method needs to be elaborated. In the future, a method should be found to extend the analysis to bore groups and the complex interaction between them. Also, the study should be extended to other geometries and individual overtopping to eventually being able to predict the forces on storm walls based on the individual incoming wave and structural parameters.

ACKNOWLEDGEMENT

We gratefully acknowledge the work done by the technical staff at Ghent University to equip the wave flume with the model, the instrumentation and assisting during the operation of the model tests. The availability of the L~Davis software for the analysis of force measurements is also acknowledged.

REFERENCES

Allsop, N.W.H. et al., 2004. Safety under wave overtopping - how overtopping processes and hazards are viewed by the public, 29th International conference on coastal engineering (ASCE), Lisbon, Portugal, 12 pp.

Allsop, N.W.H. et al., 2005. Hazards to people and property from wave overtopping at coastal structures, Proceedings coastlines, structures breakwaters (ICE), 13 pp.

Chen, X. et al., 2012. Hydrodynamic load on the building caused by overtopping waves, Proceedings of 33rd International conference on coastal engineering, Santander, Spain, 11 pp.

Chen, X., Hofland, B., Altomare, C., Suzuki, T. and Uijttewaal, W., 2015. Forces on a vertical wall on a dike crest due to overtopping flow,Coastal Engineering, 95, pp. 94-104.

Chen, X., Hofland, B., Altomare, C. and Uijttewaal, W., 2014. Overtopping flow impact on a vertical wall on a dike crest, 34th International conference on coastal engineering, Seoul, Korea, 10 pp.

Cuomo, G., Allsop, W. and Takahashi, S., 2010. Scaling wave impact pressures on vertical walls. Coastal Engineering, 57, 6, pp. 604-609.

De Rouck, J. et al., 2012. Full scale impact tests of an overtopping bore on a vertical wall in the large wave flume (GWK) in Hannover, Coastal Engineering, 33, 11 pp.

Endoh, K. and Takahashi, S., 1994. Numerically modeling personnel danger on a promenade breakwater due to overtopping waves, International conference on coastal engineering, Kobe, Japan, pp. 1017-1029.

Geeraerts, J. et al., 2005. Hazards from wave overtopping: Field measurements on the zeebrugge breakwater, Proceedings second International Coastal Symposium (ICS), Hornafjörður, Iceland, 14 pp.

Hughes, S.A., Thornton, C.I., Van der Meer, J.W. and Scholl, B.N., 2012. Improvements in describing wave overtopping processes, International conference on coastal engineering, Santander, Spain, 15 pp.

IPCC, 2014. Climate change 2014: Synthesis report. Contribution of working groups I, II and III to the fifth assessment report of the intergovernmental panel on climate change [core writing team, r.K. Pachauri and L.A. Meyer (eds.)]. IPCC, Geneva, Switzerland, 151 pp.

Kortenhaus, A. and Oumeraci, H., 1998. Classification of wave loading on monolithic coastal structures. International conference on coastal engineering, Copenhagen, Denmark, pp. 867-880.

Mansard, E.P.D. and Funke, E.R., 1980. The measurement of incident and reflected spectra using a least squares method, International conference on coastal engineering, Hamburg, Germany, pp. 154-169.

Martin, F.L., Losada, M.A. and Medina, R., 1999. Wave loads on rubble mound breakwater crown walls, Coastal Engineering, 37, 2, pp.149-174.

Mertens, T. et al., 2008. An integrated masterplan for flanders future coastal safety, 7 pp.

Oumeraci, H., Klammer, P. and Partenscky, H., 1993. Classification of breaking wave loads on vertical structures, Journal of Waterway, Port, Coastal, and Ocean Engineering, 119, 4, pp. 381-397.

Ramachandran, K. et al., 2012. Loading of vertical walls by overtopping bores using pressure and force sensors- a large scale model study, Coastal Engineering, 33, 15 pp.

Ramsden, J.D., 1996. Forces on a vertical wall due to long waves, bores and dry-bed surges, Journal of Waterway, Port, Coastal, and Ocean Engineering, 122, 3, pp. 134-141.

Schüttrumpf, H. and Oumeraci, H., 2005. Layer thicknesses and velocities of wave overtopping flow at seadikes, Coastal Engineering, 52, 6, pp. 473-495.

UNEP, 2006. Marine and coastal ecosystems and human well- being: A synthesis report based on the findings of the millenium ecosystem assessment, 80 pp.

Van der Meer, J.W., Hardemann, B., Gosse-Jan, S., Schüttrumpf, H. and Verheij, H., 2010. Flow depths and velocities at crest and landward slope of a dike. In theory and with wave overtopping simulator, 32nd international conference on coastal engineering, Shanghai, China, 15 pp.

Van Doorslaer, K., De Rouck, J., Van der Meer, J.W. and Trouw, K., 2012. Full scale wave impact tests on a vertical wall using the wave overtopping simulator, 6 pp.

Verwaest, T. et al., 2011. Hydrodynamic loading of wave return walls on top of seaside promenades. 6th International conference on coastal structures, Yokohama, Japan, pp. 568-576.